# Template self-assembly of polyiodide networks

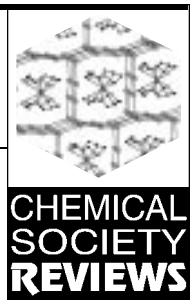


**Alexander J. Blake,[a] Francesco A. Devillanova,[b] Robert O. Gould,[c] Wan-Sheung Li,[a] Vito Lippolis,[a] Simon Parsons,[c] Christian Radek[c] and Martin Schröder*[a]**

[a] *Department of Chemistry, The University of Nottingham, Nottingham, UK NG7 2RD*
[b] *Dipartmento di Chimica e Tecnologie Inorganiche e Metallorganiche, University of Cagliari, Via Ospedale 72, 09124 Cagliari, Italy*
[c] *Department of Chemistry, The University of Edinburgh, Edinburgh, UK EH9 3JJ*

**A range of metal thioether macrocyclic complexes has been used as templating agents in the preparation of extended multi-dimensional polyiodide arrays. A selection of unusual and intriguing polyiodides is described, and the role played by the size, shape and charge of the metal macrocyclic complex discussed.**

*Alexander J. Blake received both his BSc and PhD degrees in Chemistry from Aberdeen University, where he was first introduced to crystal structure determination. Following a period of postdoctoral work at Exeter University he moved to the Chemistry Department at the University of Edinburgh in 1982, initially to develop new methods for the study of low-melting compounds by single crystal X-ray diffraction. From 1985 he took over responsibility for the running of the Department's Crystal Structure Service as a Staff Crystallographer. He has been a Co-Editor of* Acta Crystallographica *since 1995 and in August of that year moved to the Chemistry Department of the University of Nottingham where he is currently a Research Officer and the Manager of the Crystal Structure Service. Research interests include supramolecular structure and the exploitation of low-temperature techniques for crystallographic data collection.*

*Francesco A. Devillanova graduated in Chemistry at the University of Bari in 1964. In the same year he moved to the University of Modena as temporary Professor of General and Inorganic Chemistry. In 1972 he moved to the University of Cagliari where in 1980 he was appointed to the Chair of Inorganic Chemistry. His scientific interests focus on sulfur and selenium chemistry and on the donor–acceptor interaction between chalcogen donors and transition metal ions, halogens and interhalogens.*

*Robert O. Gould was an undergraduate at Williams College, Williamstown, Mass and gained his PhD from Queen's College Dundee (University of St. Andrews) under the supervision of Dr R. F. Jameson in 1963. He was appointed to the staff in the Chemistry Department, University of Edinburgh in 1962 and was subsequently promoted to lecturer (1964), Senior Lecturer (1985) and Reader (1997). His research interests are primarily in the study of complexes by X-ray diffraction, and to improving methods of crystal structure determination.*

*Wan-Sheung Li gained both her BSc and PhD degrees at the University of North London. The latter, under the supervision of Professor Mary McPartlin, was devoted to the study of homo- and hetero-nuclear metal–metal bonded complexes. In early 1996 she took up a postdoctoral position in the Department of Chemistry of the University of Nottingham where she was involved in the running of the Departmental Crystal Structure Service. In January 1998 she took up a position in the Computational Chemistry Group within the Institute of Chemistry, Academia Sinica, Taipei, Taiwan.*

*Vito Lippolis graduated in Chemistry in 1991 at the University of Pisa and in the same year gained a Diploma in Chemistry at the 'Scuola Normale Superiore' of Pisa. In 1992 he was appointed permanent researcher in Inorganic Chemistry at the University of Cagliari. He is currently a 2nd year PhD student at the University of Nottingham under the supervision of Professor Martin Schröder.*

*Simon Parsons gained a BSc Degree in 1987 from the University of Durham and PhD in Chemistry in 1991 from the University of New Brunswick, Canada under the supervision of J. Passmore. After postdoctoral research at the University of Oxford (with A. J. Downs), he was appointed to a postdoctoral position in crystallography at the University of Edinburgh in 1993. In 1995 he was appointed Staff Crystallographer in the same Department.*

*Christian Radek gained his first degree (1990) from the Ruhr-University, Bochum and carried out his Diplom-arbeit with Professor Karl Wieghardt. He was awarded his PhD from the University of Edinburgh under the supervision of Professor Martin Schröder in 1995, and is currently studying for a degree in Economics at the Hogeschool van Utrecht.*

*Martin Schröder gained a BSc Degree in Chemistry from the University of Sheffield in 1975, and a PhD in Inorganic Chemistry from Imperial College, London under the supervision of W. P. Griffith in 1978. After postdoctoral research at the ETH, Zürich (with A. Eschenmoser) and Cambridge (with J. Lewis), he was appointed in 1982 to a Demonstratorship in Inorganic Chemistry at the University of Edinburgh. He was subsequently promoted in Edinburgh to lecturer, reader, and in 1994 to a personal chair in Inorganic Chemistry. In 1995 he was appointed to the Chair and Head of Inorganic Chemistry at the University of Nottingham. He has been awarded the Corday Morgan Medal and Prize of the Royal Society of Chemistry, and a Royal Society of Edinburgh Support Research Fellowship.*

## 1 Introduction

It is well known that the heavier halogens can form oligomeric catenated cations and anions.[1] Since $I_2$ exhibits the highest tendency to form stable catenated anionic species,[1] the synthesis and structural characterisation of polyiodides continue to be an active area of investigation. Recent interest in this aspect of the chemistry of $I_2$ comes from its use as an acceptor in the synthesis of mixed-valence donor–acceptor materials which exhibit unusual electrical behavior.[2] The resulting polyiodide species fit favourably in the crystal lattice of these materials by occupying one-dimensional channels within stacks of partially oxidized donor molecules.

Numerous examples of small polyiodides such as $I_3^-$, $I_4^{2-}$ and $I_5^-$ have been reported, but relatively few extended and very extended discrete oligomeric anionic polyiodides such as $I_7^-$,[3–7] $I_8^{2-}$,[8–11] $I_9^-$,[12] $I_{10}^{4-}$,[13] $I_{12}^{2-}$,[14,15] $I_{16}^{2-}$,[15] $I_{16}^{4-}$,[16] $I_{22}^{4-}$,[17] and $I_{29}^{3-}$[18] have been characterised structurally. Although these higher polyiodides can all be described on the basis of crystallographic structural data and spectroscopic studies[19] as a combination of perturbed (slightly elongated) $I_2$ molecules [I–I = 2.75–2.80 Å] with long-range interactions to $I_3^-$ and $I^-$ ions [I···I = 3.4–3.6 Å], their geometrical features can be very different. '**Z**' and '**S**'-shaped chains have been found for $I_8^{2-}$[8] and $I_{16}^{4-}$[16] units respectively; a '**T**'-bonding motif has been observed for $I_9^-$[12] whereas for $I_7^-$ different arrangements, from a twisted ladder in *N*-methyl-γ-picolinium heptaiodide[20] to a trigonal pyramidal shape in the iodonium salt [(*N*-methylbenzothiazole-2(3*H*)-thione)$_2$I]$I_7$,[5] have been reported. Thus, variation of the counter-cation leads to variation in counter-anion structures. Some of these polyiodides are present in the crystal lattice as discrete aggregates but they frequently tend to form polymeric one-dimensional chain structures or infinite three-or two-dimensional networks[15,21–24] in which the identification of the basic polyiodide unit becomes arbitrary. In these cases the polyiodide arrays form 'unusual supramolecular inorganic matrices' (ref. 25 in ref. 15) and are better described as aggregates of $I_2$, $I^-$ and $I_3^-$ entities held together by I···I bonding interactions of varying strengths, from rather strong [*ca.* 3.4 Å] to fairly weak [*ca.* 4.1 Å].

Some authors have recognised the nature (shape, size and charge) of the cation as playing a crucial role on the structural and geometrical features of the associated polyiodide species. For example, small cations in the crystal lattice tend to be associated with asymmetric $I_3^-$ ions, whereas larger cations seem to induce a symmetrical shape.[25] It is commonly accepted that large anions are stabilised best by large cations and Mertes *et al.*[9,26] recognised the use of bulky metal macrocyclic complexes for the stabilization of unusual extended polyiodide species. They expected that the steric properties of the chosen aza-macrocyclic ligand would be more important than the nature of the metal ion in determining the nature of polyiodide ion. Indeed, macrocyclic thioether complexes seem to be ideal reaction partners in the preparation of oligomeric anionic polyiodides since they are relatively chemically inert and their size, shape and charge can be fine-tuned by changing either the metal ion or the thioether ligand. Furthermore, thioether macrocycles are known as free ligands to form a range of charge-transfer (CT) adducts with $I_2$.[27]

We describe in this review the synthesis and structures of a selection of unique polyiodide arrays using thioether macrocycle complexes[28] as templating agents. For some of these structures, it has been found necessary to consider I···I non-bonding contacts of lengths similar to the sum of the van der Waals radii for $I_2$ [4.3 Å] in order to allow adequate description of the polyiodide lattice. The discussion has been organised into two sections. The first, dealing with structural results, has been divided into several subsections according to the chemical formula of the starting template metal macrocyclic complex used for the formation of the polyiodide array. In the second section, an overview will be given of the information obtainable from the use of the FT-Raman spectroscopy in the characterisation of polyiodide species; finally, this background will be used to interpret the FT-Raman spectra of the polyiodides described.

## 2 Structural characterisation

### 2.1 [Ag([15]aneS$_5$)]BF$_4$ ([15]aneS$_5$ = 1,4,7,10,13-pentathiacyclopentadecane)

The co-ordination chemistry of $Ag^I$ with [15]aneS$_5$ has already attracted some attention because of the predicted stereochemical mismatch between the co-ordination preferences of the $Ag^I$ ion (octahedral or tetrahedral) and the macrocycle (five co-ordinate). The structure of the [Ag([15]aneS$_5$)]$^+$ cation has been found to be dependent upon the nature of the counter-anion[29] and we thought that this structural flexibility might be a useful attribute in a templating agent for polyiodide anions.

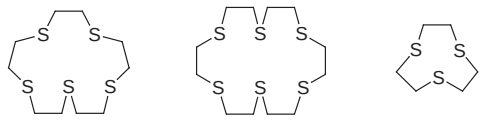

[15]aneS$_5$ [18]aneS$_6$ [9]aneS$_3$

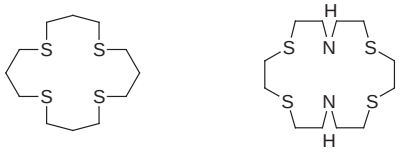

[16]aneS$_4$ [18]aneN$_2$S$_4$

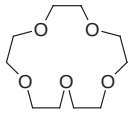

[15]aneO$_5$

#### *2.1.1 [Ag$_2$([15]aneS$_5$)$_2$]I$_{12}$*

Reaction of [Ag([15]aneS$_5$)](BF$_4$) (prepared *in situ* from [15]aneS$_5$ and AgBF$_4$) with three molar equivalents of $I_2$ in MeCN and slow evaporation of the solvent affords dark red plates. An X-ray crystal structure determination shows[30] the asymmetric unit to consist of two independent [Ag([15]aneS$_5$)]$^+$ cations and a discrete $I_{12}^{2-}$ polyiodide anion interacting with each other through Ag–I bonds, the two cations being located on the same side of the polyiodide anion (Fig. 1). The $Ag^I$ ions are four co-ordinate with a very distorted tetrahedral geometry. Only three of the five potential S-donor atoms of the macrocyclic ligand are co-ordinated to each $Ag^I$ ion [Ag–S = 2.593(6)–2.783(6) Å] and the fourth co-ordination site is occupied by an $I^-$ ion [Ag–I = 2.781(3), 2.830(3) Å].

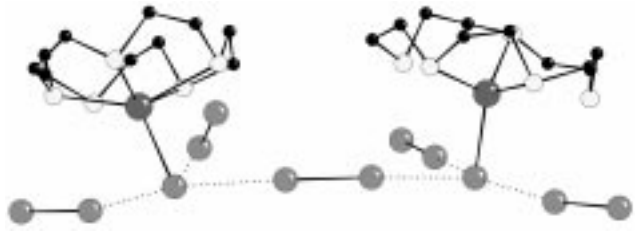

**Fig. 1** View of [Ag([15]aneS$_5$)]$_2$I$_{12}$. The asymmetric unit consists of two independent [Ag([15]aneS$_5$)]$^+$ cations and a discrete $I_{12}^{2-}$ polyiodide anion.

The $I_{12}^{2-}$ polyiodide anion can be viewed as an almost linear $I_4^{2-}$ unit interacting at each of its termini with two di-iodine molecules to give an overall twisted 'H' configuration (Fig. 1)

(the twisting angle between the two peripheral $I_2\cdots I^-\cdots I_2$ fragments is *ca.* 40.3°). The $I_4^{2-}$ unit is built up from one di-iodine molecule and two $I^-$, and consequently the overall $I_{12}^{2-}$ polyiodide is best described as $[2I^-\cdot 5I_2]$. The I–I bond distances in the perturbed $I_2$ molecules [2.755(2)–2.770(2) Å] are longer than that in $I_2$ in the vapour [2.667(2) Å] or in the solid state [2.715(6) Å].[19] This elongation is attributable to donation of electron density from $I^-$ to the σ*-antibonding LUMO of the $I_2$ molecules with $I^-\cdots I$–I contacts ranging from 3.242(2) to 3.563(2) Å.

$I_{12}^{2-}$ polyiodides are quite rare in the literature, with only four examples being reported: $[K(Crypt\text{-}2.2.2)]_2I_{12}$,[14] $(Me_2Ph_2N)_2I_{12}$,[15] $[Cu(dafone)_3]I_{12}$ (dafone = 4,5-diazafluoren-9-one),[31] and $(MePh_3P)_4I_{22}$.[17] In these compounds the $I_{12}^{2-}$ polyiodides are crystallographically centrosymmetric and consist of two pentaiodide groups bridged through their central $I^-$ by di-iodine molecules [$I_5^-\cdots I_2$ = 3.360(2)–3.481(2) Å]; in the last compound two further end-on interacting pentaiodides [$I_5^-\cdots I_2$ = 3.667(2) Å] give rise to an overall discrete $I_{22}^{4-}$ ion. In $[Ag_2([15]aneS_5)_2]I_{12}$ an extended three-dimensional superstructure is built up *via* a network of additional I···S interactions with the terminal iodine atoms [I(1), I(2), I(3) and I(4) in Fig. 2]

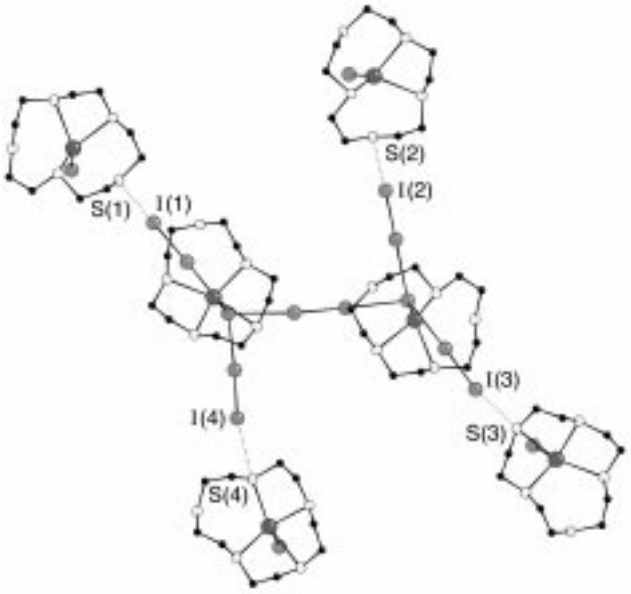


**Fig. 2** View of $[Ag_2([15]aneS_5)_2]I_{12}$. I···S interactions link adjacent asymmetric units. I(1)···S(1) = 2.987(6), I(2)···S(2) = 3.131(6), I(3)···S(3) = 3.056(6), I(4)···S(4) = 3.498(6) Å.

of each $I_2$ unit interacting with one S-donor atom of four adjacent $[Ag([15]aneS_5)]^+$ cations. These interactions involve sulfur atoms unco-ordinated to $Ag^I$ [I···S = 2.987(6)–3.131(6) Å] and sulfur atoms already bound to the metal ion [I···S = 3.498(6) Å], and generate spirals of $I_{12}^{2-}$ and $[Ag([15]aneS_5)]^+$ ions which alternate through the crystal lattice along the (001) direction with a distorted square projection in the (110) plane (Fig. 3).

### 2.2 $[Ag([18]aneS_6)]BF_4$, $[Ag([9]aneS_3)_2]BF_4$ ([18]aneS$_6$ = 1,4,7,10,13,16-hexathiacyclooctadecane, [9]aneS$_3$ = 1,4,7-trithiacyclononane)

Our postulate that the shape and the charge of the cation might play the main role in the assembly of the polyiodide anions led us to investigate $[Ag([18]aneS_6)]^+$ and $[Ag([9]aneS_3)_2]^+$ as potential templates. The charge on these cations is the same as for $[Ag([15]aneS_5)]^+$ but the shape is very different, with $[Ag([18]aneS_6)]^+$ and $[Ag([9]aneS_3)_2]^+$ regarded as essentially spherical. Furthermore, these $Ag^I$ cations are octahedral and therefore co-ordinatively saturated with no further co-ordination sites available for $I^-$ ions. The structures of the $[Ag([18]aneS_6)]^+$ and $[Ag([9]aneS_3)_2]^+$ cations have been

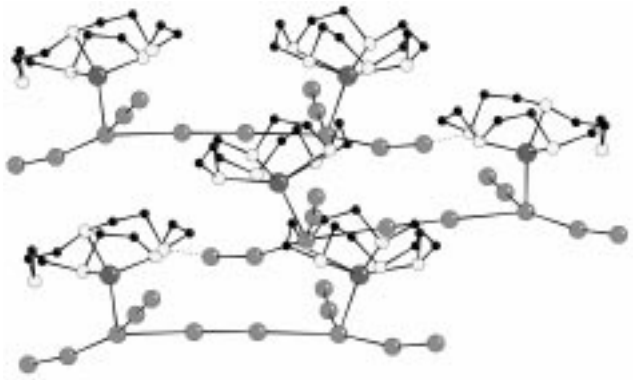

**Fig. 3** View of $[Ag([15]aneS_5)]_2I_{12}$. Alternating $I_{12}^{2-}$ anions and $[Ag([15]aneS_5)]^+$ cations spiral along the (001) direction

reported previously[28] and show the $Ag^I$ ion to have trigonally distorted octahedral co-ordination geometries.

Reaction of $[Ag([18]aneS_6)]BF_4$ with three molar equivalents of $I_2$ in $CHCl_3$–$MeNO_2$ (8 : 5 v/v) affords, after the evaporation of the solvent *in vacuo*, a dark-blue powder presumed to be $[Ag([18]aneS_6)]I_5$. Re-crystallisation of this product from MeCN and EtOH gives deep red crystals of $[Ag([18]aneS_6)]I_7$ and brown crystals of $[Ag([18]aneS_6)]I_3$ respectively. $[Ag([18]aneS_6)]I_3$ can also be prepared by metathesis of $[Ag([18]aneS_6)]BF_4$ with $Bu_4NI_3$, while addition of two molar equivalents of $I_2$ to $[Ag([18]aneS_6)]I_3$ affords $[Ag([18]aneS_6)]I_7$ in high yield. Likewise, the reaction of $[Ag([9]aneS_3)_2]BF_4$ with $I_2$ in MeCN affords $[Ag([9]aneS_3)_2]I_5$, crystals of which have been isolated by slow evaporation of the solvent.

#### *2.2.1 $[Ag([18]aneS_6)]I_7$*

The single crystal structure of $[Ag([18]aneS_6)]I_7$[32] shows the $[Ag([18]aneS_6)]^+$ cations embedded in a three-dimensional polymeric polyiodide matrix of $I_7^-$ anions (Fig. 4). The overall

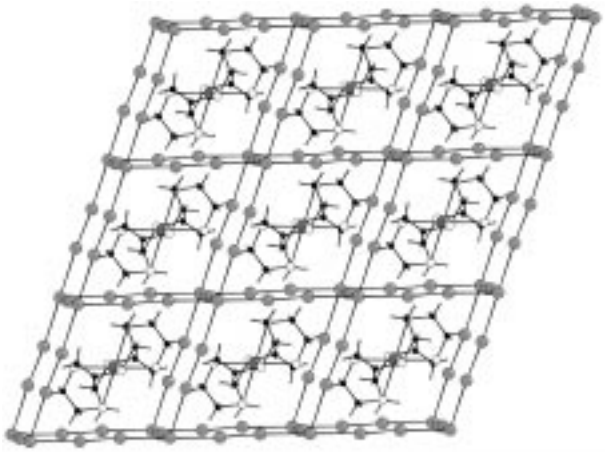

**Fig. 4** View of $\{[Ag([18]aneS_6)]I_7\}_\infty$

structure of the $[I_7^-]_\infty$ network can best be described as a distorted cube in which $I^-$ ions occupy the lattice points of a primitive rhombohedral lattice with one slightly elongated $I_2$ molecule [I–I = 2.7519(14) Å] placed along each edge, bridging two $I^-$ ions, [$I^-\cdots I_2$ = 3.3564(15) Å]. Each cube edge in this unique three-dimensional network (Fig. 5) consists therefore of an $I^-\cdots$I–I$\cdots I^-$ arrangement and each $I^-$ interacts with six molecules of $I_2$ with a local $D_{3d}$ symmetry.

None of the previously reported $I_7^-$ polyiodide species exhibit a comparable cube-like structure. Before 1991, only two structurally characterised heptaiodide ions, namely $[NEt_4]I_7$[23] and $[(py)_2I]I_7$[24] were known. Both of these show three-dimensional networks of symmetrical $I_3^-$ anions and $I_2$

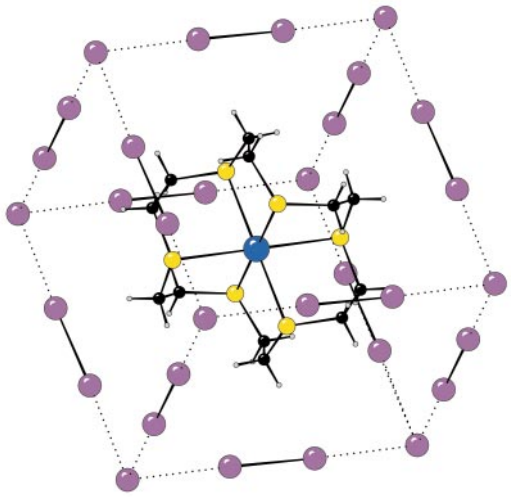

**Fig. 5** View of one cube-like array in $\{[Ag([18]aneS_6)]I_7\}_\infty$

molecules and are best described as adducts of the type $[I_3^-\cdot(I_2)_2]$. In 1992 Poli *et al.* reported[4] the crystal structure of $[PPh_4]I_7$ as the first example of a discrete $I_7^-$ ion, but the presence of a significantly asymmetric $I_3^-$ unit [I–I = 2.814(1), 3.07(1) Å] means that the $[I_3^-\cdot(I_2)_2]$ description cannot be ruled out. The same might be said of the trigonal pyramidal heptaiodides in $EtPh_3PI_7$ and $Bipy\cdot HI_7$ reported by Tebbe *et al.*,[21,22] the latter being better described perhaps as $[I_5^-\cdot I_2]$ rather than $[I_3^-\cdot(I_2)_2]$ or $[I^-\cdot(I_2)_3]$ because of the pattern in the bonding-interactions between the central $I^-$ and the three perturbed di-iodine molecules [$I^-\cdots\underline{I}$ = 3.089(3), 3.094(4), 3.440(4) Å]. In 1993, Devillanova *et al.* reported[5] the first example of an $I_7^-$ ion—in [(*N*-methylbenzothiazole -2(3*H*)-thione)$_2$I]$I_7$—which is a genuine $[I^-\cdot(I_2)_3]$ adduct. This has approximate $C_{3v}$ symmetry and I–I distances within the three perturbed $I_2$ molecules ranging from 2.746(1) to 2.771(1) Å; the three $I^-\cdots\underline{I}$ interactions lie in the range 3.237(1)–3.260(1) Å. Only three other $I_7^-$ ions with the same trigonal pyramidal geometry are known. In $(Hpy)_2I_7I_3$,[3] [Cu(OETTP)]$I_7$[6] and [$(H_3O^+\cdot$18-crown-6)]$I_7$[7] one of the three $I^-\cdots\underline{I}$ interactions is either much longer or much shorter than the other two, with a distance in the range 3.154(9) to 3.354(3) Å. These $I_7^-$ anions can still be described as $[I^-\cdot(I_2)_3]$ adducts but with approximate $C_s$ symmetry. The $I_7^-$ anions in $(Hpy)_2I_7I_3$,[3] and [$(H_3O^+\cdot$18-crown-6)]$I_7$,[7] like the one in [(*N*-methylbenzothiazole-2(3*H*)-thione)$_2$I]$I_7$[5] are characterised by head-to-tail long-range interactions [3.426(3)–3.545(13) Å] of the $I^-$ of one $I_7^-$ unit with an $I_2$ molecule of the next to give infinite one-dimensional chains.

The template effect of the $[Ag([18]aneS_6)]^+$ cation in the formation of the unique cubic $[I_7^-]_\infty$ structure may be rationalised by comparing the diagonals of the cube of iodines with the spacing of the $S_3$ triangles making up the faces of the distorted co-ordination octahedron around $Ag^I$. The diagonal along the threefold axis of the cation is 11.850 Å, while the other diagonals are 17.635 Å. The thickness of the cation may be estimated as the separation of the $S_3$ triangles [2.48 Å] plus twice the van der Waals radius of the sulfur [1.85 Å], giving 6.18 Å. Its mean diameter may be considered as twice the mean distance of the carbon atoms from the threefold axis [3.55 Å] plus twice the van der Waals radius of carbon [1.50 Å], giving 10.10 Å. Therefore the $[Ag([18]aneS_6)]^+$ cations fit very well into the cubic second-sphere polyiodide framework. Conceptually, therefore, the formation of the cube-like $[I_7^-]_\infty$ matrix may be regarded as a second-sphere template reaction around a central metal-complex cation.

*2.2.2 [Ag([18]aneS$_6$)]I$_3$*

The structure of this complex shows $[Ag([18]aneS_6)]^+$ cations and symmetrical $I_3^-$ ions [I–I 2.9137(3) Å] in the crystal lattice.[32] Fig. 6 shows parallel stacks of macrocycle complexes and $I_3^-$ ions. This $I_3^-$ salt may be considered a structural precursor to $[Ag([18]aneS_6)]I_7$ *via* the addition of two equivalents of $I_2$ to $[Ag([18]aneS_6)]I_3$. Thus, addition of $I_2$ to $[Ag([18]aneS_6)]I_3$ converts a one-dimensional (1D) lattice of $I_3^-$ to 2D and 3D lattices of $I_5^-$ and $I_7^-$ respectively. Unfortunately, we have thus far been unable to crystallise the $I_5^-$ salt of $[Ag([18]aneS_6)]^+$ due to its relative instability.

**Fig. 6** The single crystal structure of $[Ag([18]aneS_6)]I_3$; packing diagram in the (110) plane

It is important to note the different structural modifications of the $[Ag([18]aneS_6)]^+$ cation observed in $[Ag([18]aneS_6)]PF_6$, $[Ag([18]aneS_6)]I_7$ and $[Ag([18]aneS_6)]I_3$. In all three cases the macrocyclic cation adopts a trigonally compressed octahedral geometry with S–Ag–S chelate angles of about 80° and non-chelate angles of about 100°. However, in the $I_7^-$ salt all the Ag–S distances are equivalent [2.754(2) Å], while the $PF_6^-$ salt shows a tetragonal compression [$Ag–S_{ax}$ = 2.697(5), $Ag–S_{eq}$ = 2.753(4) Å][28] and the $I_3^-$ salt a tetragonal elongation [$Ag–S_{ax}$ = 2.8007(10), $Ag–S_{eq}$ = 2.7255(7) Å].[32] The cation is therefore able to modify its shape slightly, thereby perhaps offering different templating effects to the polyiodide anion.

*2.2.3 [Ag([9]aneS$_3$)$_2$]I$_5$*

Although the $[Ag([9]aneS_3)_2]^+$ cation has potentially the same shape, dimensions and charge as $[Ag([18]aneS_6)]^+$, it does not show the same template effect: under the same reaction conditions as above it forms an $I_5^-$ salt rather than a cube-like $[I_7^-]_\infty$ polyiodide array.[30] The crystal structure shows $[Ag([9]aneS_3)_2]^+$ cations and discrete V-shaped pentaiodide units. The cation shows very similar structural features to those already reported in other salts[28] with two molecules of $[9]aneS_3$ bound facially to the $Ag^I$ metal centre, conferring a distorted octahedral arrangement of six sulfur atoms. Each $I_5^-$ unit is best described as an $[I^-\cdot(I_2)_2]$ adduct [I–I = 2.7898(9), $I^-\cdots I$ = 3.1118(9) Å, $I_2\cdots I\cdots\underline{I}$ 84.61(4)°] which is located on a plane perpendicular to the approximate threefold axis of the cation. The terminal atoms of each $I_5^-$ unit interact weakly with one sulfur atom in each of two adjacent cations [$I\cdots S$ = 3.618(2) Å] so that a sinusoidal polymeric succession of cations and $I_5^-$ ions develop along the (110) direction (Fig. 7). Each chain alternates with its inversion mate such that the chains pack efficiently. The chains themselves may be regarded as being disposed in phase even though their constituent anions and cations have been interchanged.

### 2.3 [M([16]aneS$_4$)](PF$_6$)$_2$ (M = Pd, Pt) ([16]aneS$_4$ = 1,5,9,13-tetrathiacyclohexadecane)

In our attempts to synthesise unusual polyiodide arrays by using metal macrocycle complexes as template agents, we have always obtained the metathesis product whenever $Bu^n_4NI_3$ was used as starting material. In this way $[M([9]aneS_3)_2](I_3)_2$ (M = Ni, Co, Pd), $[Pd([12]aneS_4](I_3)_2$, $[Pd([15]aneN_4)](I_3)_2$ and $[Ni([15]aneN_4)(MeCN)_2](I_3)_2$ have all been synthesised and structurally characterised.[33] All of these complexes show

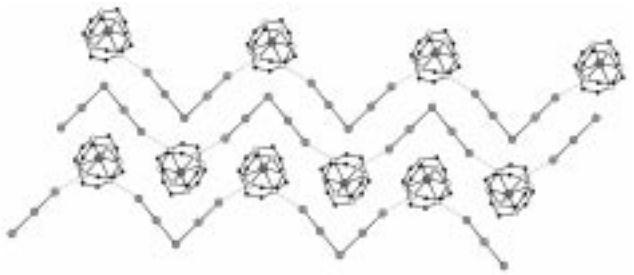

**Fig. 7** View of $[Ag([9]aneS_3)_2]I_5$. Adjacent chains are related through inversions centres and may be regarded as being in phase with each other but with the cations and anions interchanged.

isolated $I_3^-$ anions in the crystal lattice. However, in the case of $[M([16]aneS_4)](PF_6)_2$ (M = Pd, Pt) the reaction with $Bu^n_4NI_3$ in MeCN afforded unexpected products on slow evaporation of the solvent. These are isostructural and contain the binuclear cations $[([16]aneS_4)M–I–M([16]aneS_4)]^{3+}$ (M = Pd, Pt) involving a highly unusual linear M–I–M moiety in which an $I^-$ bridges two $M^{II}$ centres symmetrically (Fig. 8).[34] The M–I

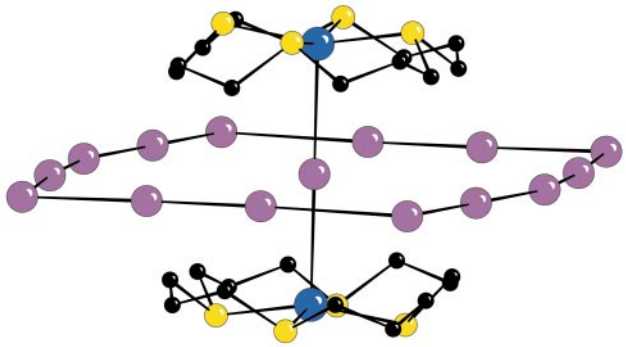

**Fig. 8** View of 14-membered polyiodide belt at the $[([16]aneS_4)Pd–I–Pd([16]aneS_4)]^{3+}$ cation template

distances are relatively long [3.135(3) for Pd and 3.194(2) Å for Pt] so the $I^-$ anion may be regarded as being trapped inside a pseudo cavity formed by two $[M([16]aneS_4)]^{2+}$ cations, with the linear M–I–M bridge being imposed by the steric bulk of the tetrathioether crown. The $[16]aneS_4$ ligand is bound *via* all four S-donors to the $M^{II}$ centres which are formally five co-ordinate in each cation. The M–S distances in $[([16]aneS_4)M–I–M([16]aneS_4)]^{3+}$ lie in the range 2.300(10)–2.315(9) Å (Pd) and 2.332(3)–2.339(3) Å (Pt) and are slightly elongated compared to those of the parent $[Pd([16]aneS_4)]^{2+}$ and $[Pt([16]aneS_4)]^{2+}$ cations.[28,35] The $Pd^{II}$ and $Pt^{II}$ centres lie 0.352 and 0.306 Å, respectively, out of the least-squares mean plane of their $S_4$ donor sets in the direction of the bridging $I^-$ ion. Interestingly, this displacement is into the methylene manifold of the macrocycle, the opposite to that observed for $[Pd([16]aneS_4)]^{2+}$ and $[Pt([16]aneS_4)]^{2+}$.[28,35]

The same counter-polyanion structure is present in both $Pd^{II}$ and $Pt^{II}$ complex crystal structures. The basic units of the polyiodide array are a $I^-$, a distorted L-shaped $I_5^-$ fragment which can be described either as $[I^-\cdot(I_2)_2]$ or as $[I_3^-\cdot I_2]$, and a highly asymmetric $I_3^-$ moiety. In fact, choosing the first description, the I–I bond distances in the two perturbed $I_2$ molecules [I(1)–I(2), I(4)–I(5)] are 2.798(2) and 2.836(2) Å whereas the associated $I^-\cdots I_2$ bond lengths are 3.409(2) [I(2)–I(3)] and 3.044(2) Å [I(3)–I(4)] respectively. The $I_2$–I(3)–$I_2$ angle is approximately 90° as normally found in discrete L-shaped $I_5^-$ units. The $I_5^-$ units are connected to each other through contacts of 3.806(2) Å between two perturbed $I_2$ molecules to form planar zig-zag polymeric chains (Fig. 9); two of these chains flank a row of cations and are linked by pairs of bond-interactions [I(5)···I(6) = 3.285(2) Å] between an iodide [I(6)] and two terminal iodine atoms from two $I_5^-$ units. Considering the reasonably short $I^-\cdots I_2$ bond lengths, an

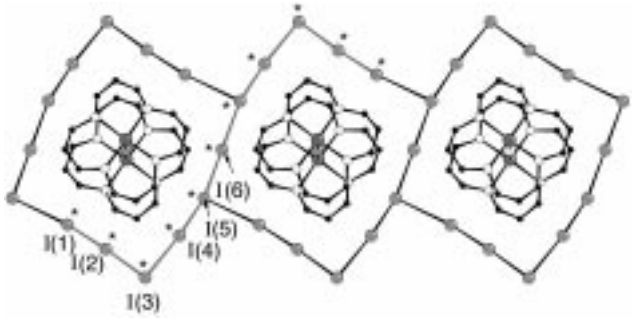


**Fig. 9** View of $[([16]aneS_4)Pd–I–Pd([16]aneS_4)]^{3+}\cdot I_{11}^{3-}$ showing the 14-membered polyiodide rings fused to give an infinite polycyclic ribbon. Starred atoms identify the basic $I_{11}^{3-}$ unit. I(1)–I(2) = 2.798(2), I(2)–I(3) = 3.409(2), I(3)–I(4) = 3.044(2), I(4)–I(5) = 2.836(2), I(5)–I(6) = 3.285(2) Å.

overall and unique $I_{11}^{3-}$ can be identified as a basic unit of the resulting polyiodide array (Fig. 9). An infinite polycyclic ribbon is therefore built up of 14-membered polyhalide rings sharing three iodine atoms. Each ring measures 9.657 by 12.640 Å (diagonal length 16.383 Å) and surrounds a binuclear metal cation with the M–I–M bridging $I^-$ placed exactly at its centre (Figs. 8 and 9). Therefore, the central complex cation may be regarded as acting as a template for the synthesis of this unique cyclic polyhalide array in which the binuclear complex cation sits.

### 2.4 $[Pd_2Cl_2([18]aneN_2S_4)](PF_6)_2$ ($[18]aneN_2S_4$ = 1,4,10,13-tetrathia-7,16-diazacyclooctadecane)

On the basis of the results obtained with $[M([16]aneS_4)](PF_6)_2$ (M = Pd, Pt), the binuclear complex $[Pd_2Cl_2([18]aneN_2S_4)](PF_6)_2$, having the same overall charge but different shape, was treated with $Bu^n_4NI_3$ in MeCN solution. After several days, two different crystal morphologies, black facetted prisms and brown elongated plates, were obtained and X-ray diffraction studies undertaken to determine their structure.

#### *2.4.1 $[Pd_2Cl_2([18]aneN_2S_4)]_{1.5}I_5(I_3)_2$*

For the black prisms, the asymmetric unit consists of one $I_5^-$ and two $I_3^-$ ions and 1.5 $[Pd_2Cl_2([18]aneN_2S_4)]^{2+}$ dications.[36] The structure of the cations is similar to that in the corresponding $PF_6^-$ salt.[37] The $Pd^{II}$ ions are each co-ordinated to one N- and two S-donor atoms, with a $Cl^-$ ligand completing the square planar co-ordination. The two co-ordination planes lie parallel to each other but the overall binuclear dication adopts a stepped conformation in order to minimise steric interactions. Interestingly, the dications are linked by an extensive network of hydrogen bonds between the (N)H and Cl atoms to form infinite chains in the crystal lattice [N···Cl = 3.254(14)–3.356(12), (N)H···Cl = 2.57 Å]. The intra-cation Pd···Pd distances are 4.055(2) and 4.155(2) Å while the Pd–Pd distances between adjacent cations are significantly shorter [3.449(2), 3.463(2) Å] (Fig. 10).

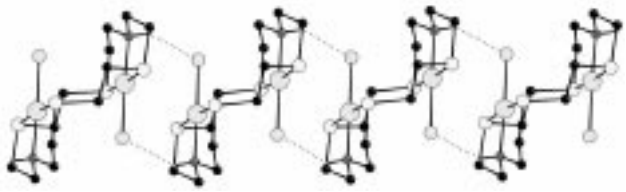

**Fig. 10** View of cation in $[Pd_2Cl_2([18]aneN_2S_4)]_{1.5}I_5(I_3)_2$

The infinite chains of binuclear dications are embedded into a unique polyiodide matrix whose fundamental units are one L-shaped $I_5^-$ ion consisting of an asymmetric $I_3^-$ [I(1)–I(2) = 2.845(2), I(2)–I(3) = 3.045(2) Å, < I(1)–I(2)–I(3) = 179.69(9)°] and a di-iodine molecule [I(10)–I(11) = 2.775(3) Å] linked by I(3)–I(10) = 3.349(2) Å and forming an I(2)–I(3)–

I(10) angle of 90.00(6)°, and two slightly asymmetric $I_3^-$ ions [I(4)–I(5) = 2.904(2), I(5)–I(6) = 2.959(2) Å, I(4)–I(5)–I(6) = 176.47(6)°; I(7)–I(8) = 2.948(2), I(8)–I(9) = 2.929(2) Å, I(7)–I(8)–I(9) = 171.58(5)°]. The $I_3^-$ ions, including those belonging to the $I_5^-$ units, lie on parallel planes and form unprecedented continuous planar two-dimensional layers. Each layer [Fig. 11(*a*)] consists of alternating fused ribbons of 14-membered and 24-membered rings with contacts among the $I_3^-$ ranging from 3.758(2) to 4.217(2) Å. Pairs of parallel $I_2$ molecules [$I_2 \cdots \underline{I}_2$ = 4.257(2) Å] from two symmetry-related $I_5^-$ fragments lie orthogonal to the two-dimensional layers and connect two of these by passing through the centres of the 24-membered rings of a third layer located in between them [Fig. 11(*a*) and (*b*)]. The connection of two alternating layers takes place through an $I_5^- \cdots \underline{I}_3^-$ interaction of 3.573(2) Å so that an overall $I_8^{2-}$ [shown as open circles in Fig. 11(*b*)] can be

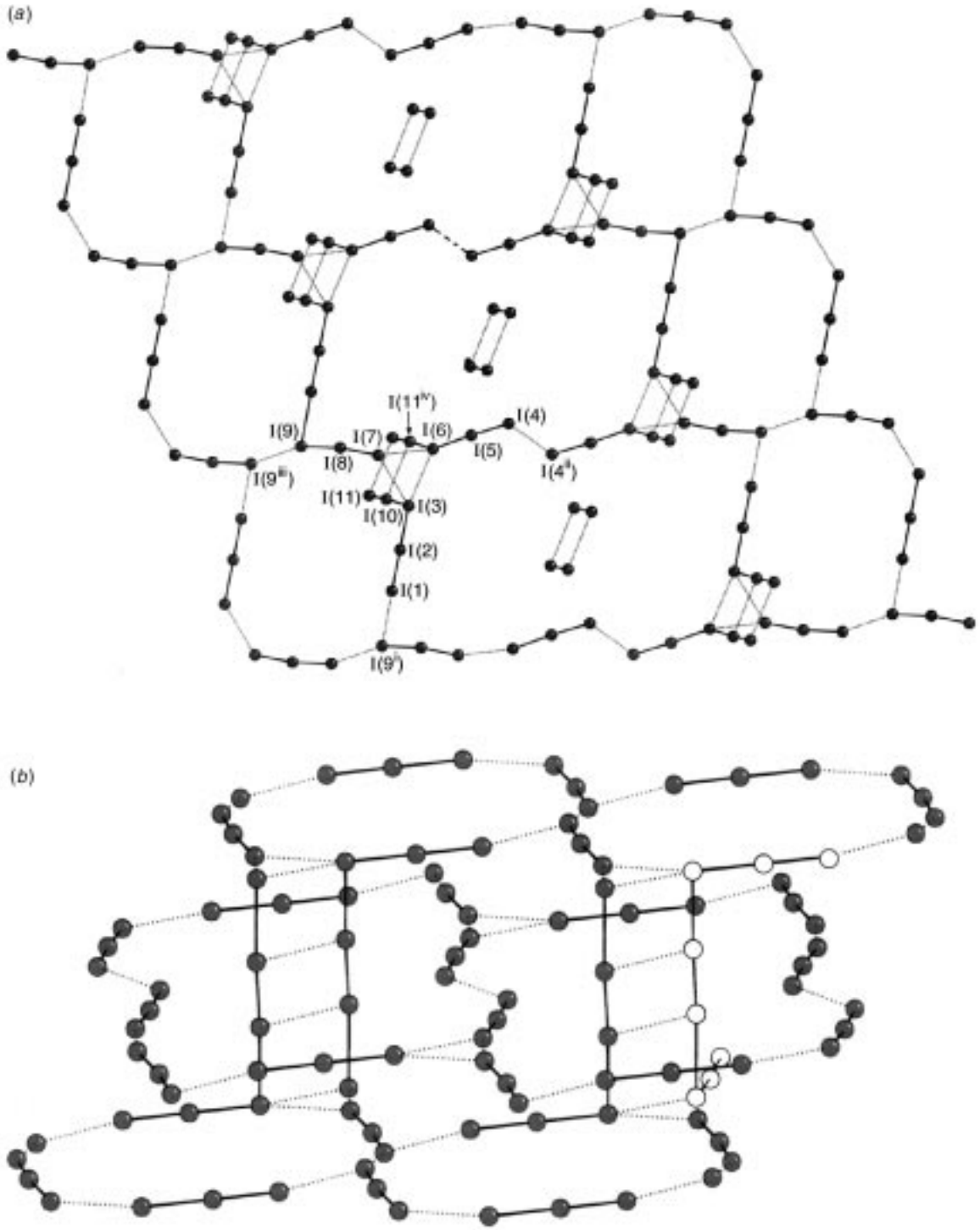


**Fig. 11** (*a*) View of polyanion in $[Pd_2Cl_2([18]aneN_2S_4)]_{1.5}I_5(I_3)_2$ showing two-dimensional layers comprising linked $I_3^-$ anions form alternating fused ribbons of 14-membered and 24-membered rings. I(1)–I(2) = 2.845(2), I(2)–I(3) = 3.045(2), I(4)–I(5) = 2.904(2), I(5)–I(6) = 2.959(2), I(7)–I(8) = 2.948(2), I(8)–I(9) = 2.929(2), I(10)–I(11) = 2.775(3), I(3)–I(10) = 3.349(2), I(3)···I(6) = 4.217(2), I(3)···I(7) = 4.184(2), I(6)···I(7) = 4.006(2), I(1)···I(9) = 3.812(2), I(4)···I(4$^{i}$) = 4.017(2), I(9)···I(9$^{ii}$) = 3.758(2), I(6)···I(11$^{iv}$) = 3.579(2) Å. Symmetry operations: i = $x-1$, $y-1$, $1+z$; ii = $1-x$, $1-y$, $1-z$; iii = $2-x$, $1-y$, $-z$; iv = $2-x$, $-y$, $1-z$. (*b*) Alternate view of polyanion in $[Pd_2Cl_2([18]aneN_2S_4)]_{1.5}I_5(I_3)_2$. The poly-$I_3^-$ layers are linked by di-iodine bridges which link two 14-membered rings through a 24-membered ring. Open circles identify the basic $I_8^{2-}$ unit.

envisaged as the yarn interlocking the infinite two-dimensional poly-$I_3^-$ sheets. The 24-membered rings of each layer measure *ca.* 25.31 × 13.31 Å: the dimensions of each half [*ca.* 12.65 × 13.31 Å] are similar to those of the 14-membered rings [*ca.* 12.18 × 14.73 Å], resulting in channels along the body diagonal of the unit cell. These channels are occupied by the chains of hydrogen-bonded binuclear complexes described above (Fig. 10) to give a pseudo-rotaxane structure (Fig. 12), and it appears that it is these chains rather than the individual dication which act as the template for the polyiodide architecture.[36]

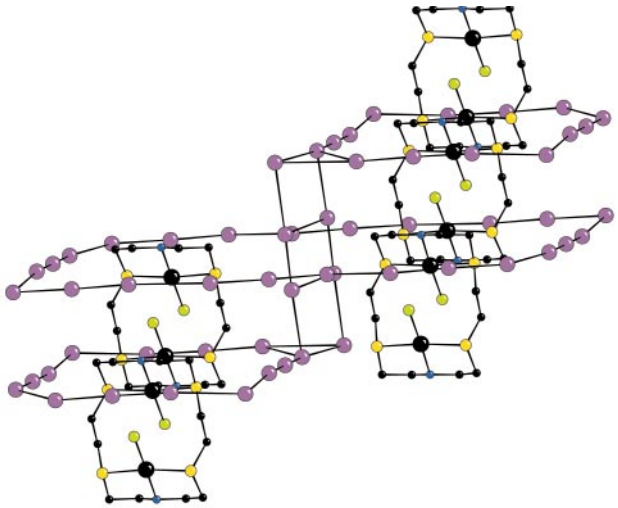

**Fig. 12** View of overall structure of $[Pd_2Cl_2([18]aneN_2S_4)]_{1.5}I_5(I_3)_2$. Chains of $[Pd_2Cl_2([18]aneN_2S_4)]^{2+}$ dications occupy channels in the three-dimensional polyiodide network in $[Pd_2Cl_2([18]aneN_2S_4)]_{1.5}I_5(I_3)_2$.

*2.4.2 $[Pd_2Cl_2([18]aneN_2S_4)](I_3)_2$*

The elongated plates obtained from the same reaction above give a much simpler structure even although the complex cation is the same.[33] The asymmetric unit consists of half of a $[Pd_2Cl_2([18]aneN_2S_4)]^{2+}$ cation and one slightly asymmetric $I_3^-$ anion [I(1)–I(2) = 2.8649(6), I(2)–I(3) = 2.9889(5) Å, < I(1)–I(2)–I(3) = 174.55(2)°]. The geometry of the dinuclear $Pd^{II}$ complex is similar to that observed in $[Pd_2Cl_2([18]aneN_2S_4)]_{1.5}I_5(I_3)_2$ but it does not generate infinite poly-cation chains through hydrogen-bonding. Instead, the $I_3^-$ ions form polymeric sinusoidal chains in the crystal lattice *via* head-to-tail $I_3^-\cdots I_3^-$ interactions of 4.0236(6) Å. These chains propagate along the (100) direction and are linked together by dinuclear Pd complex units *via* Pd···I contacts of 3.5429(6) Å [Fig. 13(*a*), (*b*)]. As shown in Fig. 13(*a*), the dications are arranged in an alternating side-to-side arrangement along the poly-$I_3^-$ chains, giving rise to infinite two-dimensional undulating layers [Fig. 13(*b*)].

**2.5 $[RhCl_2([16]aneS_4)]PF_6$**

The $Rh^{III}$ complex $[RhCl_2[16]aneS_4]^+$ allowed variation of both the overall charge of the metal cation and its shape compared to the above $Pd^{II}$ and $Pt^{II}$ complexes. In fact the presence of the two co-ordinated chloride ligands gives an overall ellipsoidal shape to the $[RhCl_2([16]aneS_4)]^+$ cation and, furthermore, does not allow interactions between the metal centre and $I^-$ or $I_2$. Such interactions are observed in the structures of $[Ag_2([15]aneS_5)_5]I_{12}$, $\{[M([16]aneS_2)]_2I\}(I_5)_2I$ (M = Pd, Pt) and $[Pd_2Cl_2([18]aneN_2S_4)](I_3)_2$ described above, and may play an important role in the overall organization of these polyiodide arrays.

The reaction of $[RhCl_2([16]aneS_4)]PF_6$ with three molar equivalents of $I_2$ in MeCN solution afforded dark, crystalline blocks after slow evaporation of the solvent. A structure determination showed the compound to have the formulation $[RhCl_2([16]aneS_4)]I_5I_2$.[33] As for its parent $PF_6^-$ complex,[28] the $Rh^{III}$ ion has a distorted octahedral geometry, being bound to all four S-donors of the thioether macrocycle in an equatorial plane and to two chloride ligands in *trans*-axial positions [Rh–S = 2.352(4)–2.361(4), Rh–Cl = 2.330(3) Å]. The $[RhCl_2([16]aneS_4)]^+$ cations are encapsulated within a three-dimensional polymeric polyiodide matrix made up of $I_5^-$ anions and slightly elongated $I_2$ molecules [I(6)–I(7) = 2.732(2) Å]. The $I_5^-$ ions consist of an asymmetric $I_3^-$ [I(3)–I(4) = 2.962(2), I(4)–I(5) = 2.884(2) Å, < I(3)–I(4)–I(5) 175.18(5)°] and a di-iodine molecule [I(1)–I(2) 2.752(2) Å] linked by I(2)–I(3) [3.172(2) Å] and forming an angle I(2)–I(3)–I(4) of 103.01(5)° (Figs. 14 and 15). Puckered anionic layers can be identified within the polyiodide network in the crystal lattice. They are composed of $I_3^-$ from the $I_5^-$ fragments and the I(6)–I(7) di-iodine molecules to form 4-, 10- and 12-membered polyiodide rings through I···I interactions of 3.336(2)–4.133(2) Å (Fig. 14). These two-dimensional infinite sheets stack along the (001) direction such that the 10-membered rings in one layer lie approximately above and below the 12-membered rings of the adjacent layers. The I(1)–I(2) molecules from the $I_5^-$ fragments link consecutive anionic layers through I···I bridging interactions of 4.106(2) Å to form very irregular cages (Fig. 15). The four vertical edges of each cage are made up of four bridging $I_2$ units, whereas the upper and lower faces each consists of one four- and one ten-membered ring. The cages have dimensions *ca.* 11.14 × 9.09 × 8.03 Å and the guest $[RhCl_2([16]aneS_4)]^+$ cation is located centrally within this cavity.

**2.6 $[K([15]aneO_5)_2]I$ ([15]aneO$_5$ = 1,4,7,10,13-pentaoxacyclopentadecane)**

In order to determine whether other types of metal macrocyclic complexes could have the same templating effect on the self-assembly of polyiodide arrays, we treated the potassium complex $[K([15]aneO_5)_2]I$ with an excess of $I_2$ in MeCN. After a few days, dark crystals were obtained by slow evaporation of the solvent. The crystal structure determination established the formulation $[K([15]aneO_5)_2]I_9$.[36] Within the cation, two molecules of the crown ether sandwich one $K^+$ ion within a ten co-ordinate environment with K–O bond distances in the range 2.62(2)–3.21(2) Å. These cations are embedded into a three-dimensional polyiodide matrix made up of nona-iodide units (Fig. 16). Each $I_9^-$ ion can be described as an $[I_3^-\cdot(I_2)_3]$ charge-transfer complex with the three perturbed $I_2$ molecules showing intermolecular distances ranging from 2.716(3) to 2.740(4) Å and interacting with the slightly asymmetric $I_3^-$ [I(7)–I(8) = 2.874(3), I(8)–I(9) = 2.978(3) Å, < I(7)–I(8)–I(9) = 178.2(1)°] through bonding contacts of 3.396(4)–3.503(4) Å. Two of the three $I_2$ molecules [I(5)–I(6) and I(3)–I(4)] and the $I_3^-$ ion [I(7)–I(8)–I(9)] lie approximately in the same plane whereas the third $I_2$ molecule [I(1)–I(2)] is perpendicular to it [ < I(1)–I(9)–I(8) = 92.4, < I(1)–I(9)–I(3) = 97.6°]. This configuration for the $I_9^-$ polyiodide ions allows them to form a three-dimensional network of puckered cube-like cages through I···I interactions of 3.732(4)–4.074(4) Å (Fig. 17). Each cage measures 9.658 × 9.521 × 9.959 Å, the diagonals across are 17.371 and 17.393 Å and the $[K([15]crownO_5)_2]^+$ cations lie almost at the centre of the cages. This polyiodide array is surprisingly similar to the ideal cubic polyiodide network in $[Ag([18]aneS_6)]I_7$, the main difference being the extra $I_2$ molecule of the $I_9^-$ ion located in the middle of the lower face of each cage reflecting the different topologies of the $Ag^I$ and $K^I$ complexes (Fig. 5 and 17). There is, therefore, a clear link between the templating of $I_7^-$ *vs.* $I_9^-$ anions. The puckered cube-like cages are arranged in a centred lattice and in projection along the crystallographic (100) axis, each cage can be seen to lie above the midpoint of four cages in the layer below. Furthermore, it is clear that the concept of self-assembly of polyiodide arrays is not restricted to transition metal thioether and aza macrocyclic complexes, but can in principle be extended to any complex cationic system.

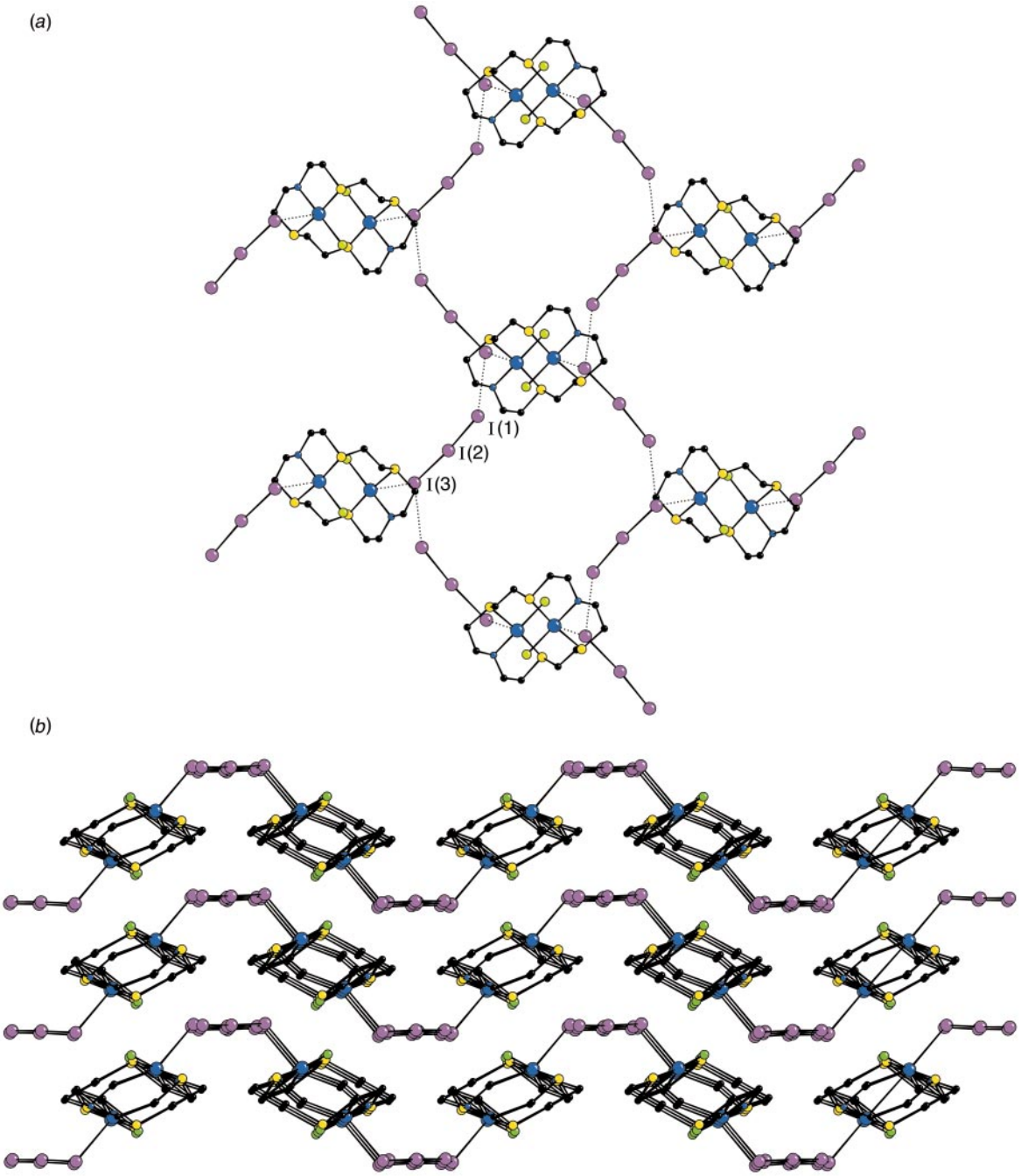


**Fig. 13** (*a*) View of $[Pd_2Cl_2([18]aneN_2S_4)](I_3)_2$ showing polymeric sinusoidal chains of $I_3^-$ ions cross-linked by $[Pd_2Cl_2([18]aneN_2S_4)]^{2+}$ dications I(1)–I(2) = 2.8649(6), I(2)–I(3) = 2.9889(5) Å. (*b*) View of $[Pd_2Cl_2([18]aneN_2S_4)](I_3)_2$, projection onto the (011) plane.

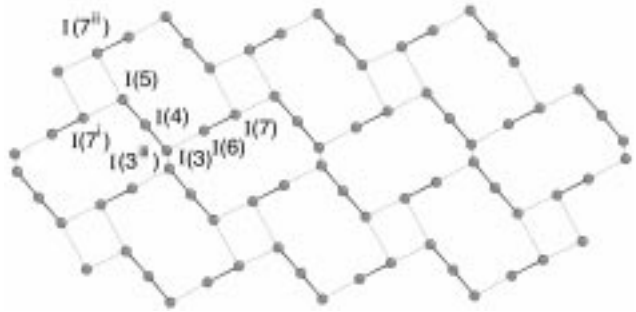


**Fig. 14** View of polyanion in $[RhCl_2([16]aneS_4)]I_5I_2$ showing the puckered anionic layer within the polyiodide network sharing 4-, 10- and 12-membered rings I(5)···I(7) = 3.336(2), I(5)···I(7$^{i}$) = 4.133(2), I(3)···I(3$^{ii}$) = 3.871(2) Å. i = $-x$, $1-y$, $-z$; ii = $x$, $-1+y$, $z$; iii = $1-x$, $1-y$, $-z$.

## 3 FT-Raman spectroscopy

When dissolved in solvents such as $CHCl_3$, $CH_2Cl_2$, $CCl_4$, and heptane, $I_2$ normally interacts with molecules (D) containing Group V and Group VI donor elements (N, P, O, S, Se) to give charge-transfer (CT) complexes *via* an acid–base equilibrium reaction.[38] In the solid state a variety of products is observed (D·$I_2$ C–T complexes, D·*n*$I_2$ C–T complexes, hypervalent compounds characterised by the I–D–I group, iodonium salts, polyiodides and mixed-valence compounds) depending upon the nature of the donor atom, the solvent and the reaction molar ratio.[5,38] This great variability of products calls for other techniques for their identification; this is particularly necessary when X-ray crystal structure determination is not available. Raman spectroscopy has been used widely for this purpose, and it provides a simple way to obtain qualitative information on the nature of iodine in the crystal lattice.

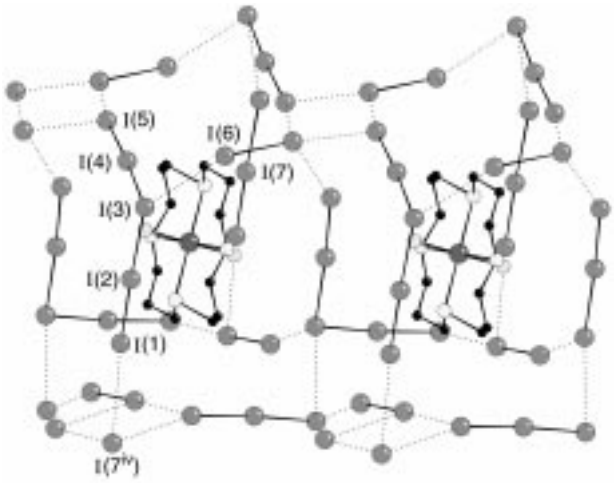


**Fig. 15** View of $[RhCl_2([16]aneS_4)]I_5I_2$ showing the puckered polyiodide cages enclosing the metal cations I(1)–I(2) = 2.752(2), I(2)–I(3) = 3.172(2), I(1)···I(7$^{iv}$) = 4.106(2), I(3)–I(4) = 2.962(2), I(4)–I(5) = 2.884(2), I(3)···I(6) = 3.776(2), I(6)–I(7) = 2.732(2) Å, iv = 1/2 + *x*, 1/2 − *y*, 1/2 + *z*

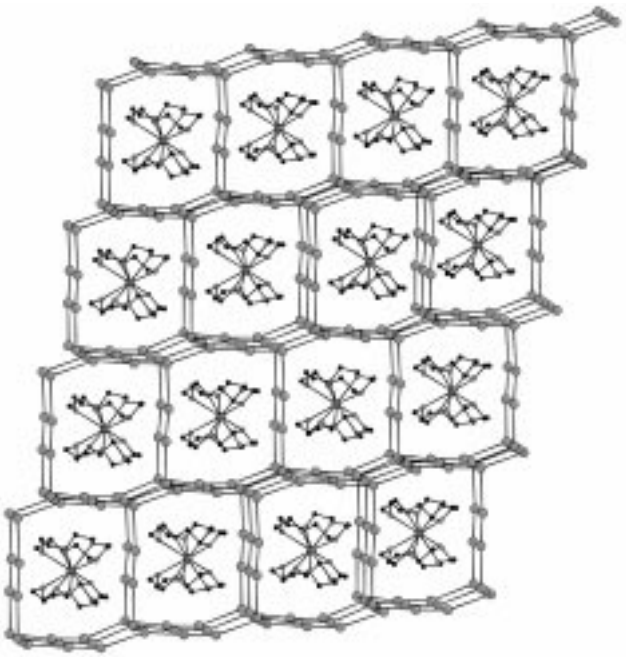

**Fig. 16** View of $[K([15]aneO_5)_2]I_9$ along the crystallographic *c* axis

In the past resonance Raman (RR) spectroscopy has been widely employed and the assignment of typical spectra to polyiodides have been generally made on model compounds which had been previously structurally characterized by X-ray diffraction.[19] However, RR uses visible laser excitation sources which may induce fluorescence, sample pyrolysis or photoreactions so that spurious peaks can appear in the spectrum.[19] This is a real possibility for polyiodides which absorb strongly in the visible region (where RR laser sources emit), and those with high iodine content are potentially prone to decomposition to give $I_2$, $I^-$ and $I_3^-$ as final products.[19] This decomposition causes changes in the Raman spectrum due to elimination of $I_2$ and the formation of $I_3^-$ which may be incorrectly assigned to the starting polyiodide material. Recently introduced Fourier transform Raman spectrometers use a near-infrared laser excitation source and thereby reduce or eliminate the above problems so that the resulting spectra can be more confidently attributed to the starting compound.[19]

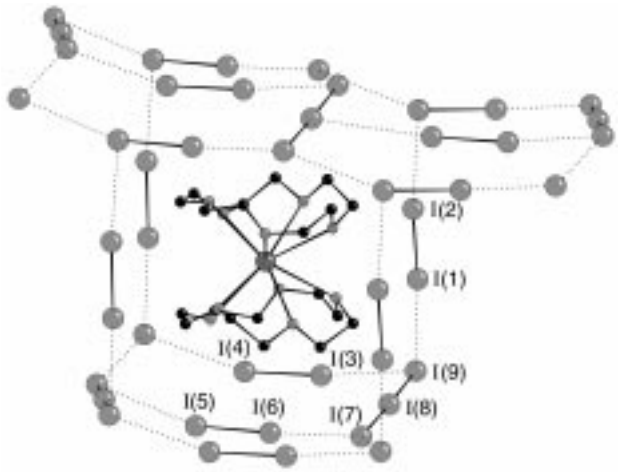


**Fig. 17** View of one polyiodide cage in $[K([15]crownO_5)_2]I_9$ I(1)–I(2) = 2.740(4), I(3)–I(4) = 2.716(3), I(5)–I(6) = 2.728(4), I(7)–I(8) = 2.874(3), I(8)–I(9) = 2.978(3), I(1)···I(9) = 3.503(4), I(3)···I(9) = 3.396(4), I(7)···I(6) = 3.346(4) Å

### 3.1 Neutral charge-transfer complexes

The ν(I–I) Raman band at 180 $cm^{-1}$ for $I_2$ in the solid state, [*d*(I–I) = 2.715 Å], is expected to move to lower frequencies when $I_2$ interacts with donor molecules to form CT-adducts. Donation of electron density occurs from a non-bonding orbital on the donor atom into the LUMO of the $I_2$ molecule: as this LUMO is an antibonding σ* orbital lying along the interatomic axis, the net bond order decreases and a longer bond distance is observed within the perturbed $I_2$ molecule. The lowering of the FT-Raman frequencies ν(I–I) upon formation of CT complex occurs for all the adducts in which the $I_2$ unit can be considered a perturbed diatomic molecule (weak or medium-weak complexes), irrespective of the nature of the donor atom. In this case a linear relationship has been found to exist between the FT-Raman frequencies ν(I–I) and the *d*(I–I) bond distances.[39] In order to differentiate weak or medium-weak adducts from strong complexes, a useful criterion is based on the value of the I–I bond order (*n*), calculated as a function of the I–I bond lengthening, according to the equation: $d = d_o - c\log n$ (*d* and $d_o$ are the I–I bond distances in co-ordinated and free $I_2$ respectively, and $c$ = 0.85 Å is an empirical constant).[39] For values of *n* higher than 0.6, the $I_2$ moiety in the CT complexes may be considered a perturbed diatomic molecule and a band in the range 180–150 $cm^{-1}$ is expected in the FT-Raman spectrum. This hypothesis is supported by the observation that polyiodides which may be described as weak or medium-weak adducts of the type $I^-\cdot(I_2)_n$ give very similar FT-Raman spectra and the recorded frequencies fit the linear correlation ν(I–I) *versus d*(I–I).[19] When the interaction between a donor molecule and $I_2$ is strong ($0.4 < n < 0.6$), as in the case of adducts with selenium-containing molecules or in symmetric triiodide, only by describing the D–I–I vibrating group as a three-body system is it possible to predict and/or assign the FT-Raman spectrum.[19]

### 3.2 Triiodides and other higher polyiodide species

In the linear and symmetric $I_3^-$ anion, the Raman-active symmetric stretch ($\nu_1$) occurs near 110 $cm^{-1}$, while the antisymmetric stretch ($\nu_3$) and the bending deformation ($\nu_2$) are only infrared-active. The latter two may also become Raman-active if a distortion of the $I_3^-$ occurs, in which case they are normally found near 130 ($\nu_3$) and 70 $cm^{-1}$ ($\nu_2$), having medium and medium-weak intensities respectively.[19,39] For highly asymmetric $I_3^-$ ions $[I^-\cdot I_2]$, as found in neutral CT adducts, the FT-Raman spectrum shows only one strong band in the range 180–150 $cm^{-1}$, indicative of a perturbed $I_2$ molecule.[39]

On the basis of structural determinations, all the higher polyiodide species (from $I_5^-$ to $I_{16}^{4-}$) may be regarded as weak or medium-weak adducts of the type $[I^-\cdot(I_2)_n]$ or $[I_3^-\cdot(I_2)_n]$. Consequently, the corresponding FT-Raman spectra will show peaks due to perturbed di-iodine molecules for $[I^-\cdot(I_2)_n]$ systems, and characteristic peaks due to both perturbed di-iodine molecules and symmetric or slightly asymmetric $I_3^-$ ions for polyiodides describable as $[I_3^-\cdot(I_2)_n]$.[39]

It is therefore evident that except for symmetric $I_3^-$ cases, the Raman technique is unable to distinguish between the different types of polyiodides or to discriminate unambiguously between the polyiodides and the neutral adducts. However, it can give valuable information on the extent of the lengthening of the I–I bond, whether or not it has been produced by interaction with a neutral donor or an ion. FT Raman spectroscopy cannot give any structural information on the nature of an extended polyiodide matrix as the technique cannot elucidate the structure beyond the basic polyiodide unit in terms of combinations of $I^-$, $I_2$ and $I_3^-$ fragments.

In Table 1 the I–I distances, the bond orders and the proposed combinations of $I^-$, $I_2$ and slightly asymmetric $I_3^-$ are collected for some polyiodides reported in the literature[19,39] as well as for the polyiodides described herein. For every compound the recorded FT-Raman spectrum is in accordance with the structural features of the basic polyiodide unit as given in the last column on the right. Further information may be extracted from the FT Raman spectrum of $[Ag([18]aneS_6)]I_7$ in which each $I^-$ interacts with six $I_2$ molecules arranged in $D_{3d}$ symmetry. Because all six $I_2$ molecules have the same I–I bond distance, only one band should be present in the FT Raman spectrum below 180 $cm^{-1}$. However, the stretching vibrations of the six individual $I_2$ units can combine and in $D_{3d}$ symmetry give rise to two Raman-active normal modes of $A_{1g} + E_g$ types. The 179 and 165 $cm^{-1}$ bands can therefore be assigned to $A_{1g}$

**Table 1** Structural and Raman parameters for some representative polyiodides and for the polyiodides arrays synthesised by using metal macrocycle complexes as templating agents

| Polyiodide anion | Compound[a] | Raman data ($cm^{-1}$)[b] | X-Ray *d*(I–I)/Å | Bond order[c] | Comments |
|---|---|---|---|---|---|
| $I_3^-$ (very asymm.) | $[(EtNH_2)dtl]I_3$[d] | 167 s | 2.714 | 0.82 | $I^-\cdot I_2$ |
| | | | 3.141 | 0.28 | |
| $I_5^-$ (bent) | $[moH]I_5$[e] | 164 s | 2.783 | 0.74 | $I_2$ |
| | | 135 m | 2.872 | 0.58 | $I_3^-$ (asymm.) |
| | | 106 mw | 2.973 | 0.44 | |
| $I_5^-$ (bent) | $[Mn(modtc)_3]I_5$[f] | 165 s | 2.750–2.759 | 0.80–0.81 | $I^-\cdot 2I_2$ |
| | | 143 s | 2.810–2.827 | 0.68–0.65 | |
| | | | 3.117–3.031 | 0.30–0.38 | |
| | | | 3.186–3.216 | 0.25–0.23 | |
| $I_7^-$ | $[bntSeMe)_2I]I_7$[g] | 175.2 m | 2.746 | 0.81 | $I^-\cdot 3I_2$ ($C_{3v}$ symm.) |
| | | 157.4 s | 2.766 | 0.77 | |
| | | | 2.771 | 0.76 | |
| $I_{16}^{4-}$ | $[mo_2ttl]_2I_{16}$[h] | 174 s | 2.741 | 0.83 | $I_2$ |
| | | 139 m | 2.858 | 0.60 | $I_3^-$ (asymm.) |
| | | 112 mw | 2.976 | 0.44 | |
| | | 161 ms | 2.827 | 0.65 | $I^-\cdot I_2$ |
| | | | 3.018 | 0.39 | |
| $I_{12}^{2-}$ | $[Ag_2([15]aneS_5)_2]I_{12}$ | 172 br s | 2.755 | 0.79 | $2I^-\cdot 5I_2$ |
| | | | 2.756 | 0.79 | |
| | | | 2.760 | 0.78 | |
| | | | 2.768 | 0.77 | |
| | | | 2.770 | 0.76 | |
| $I_5^-$ | $[Ag([9]aneS_3)_2]I_5$ | 162 s | 2.790 | 0.72 | $I^-\cdot 2I_2$ ($C_{2v}$ symm.) |
| | | 151 s | 3.112 | 0.30 | |
| $I_7^-$ | $[Ag([18]aneS_6)]I_7$ | 179 m | 2.752 | 0.80 | $I^-\cdot 3I_2$ ($D_{3d}$ symm.) |
| | | 165 s | 3.357 | 0.16 | |
| $I_5^-$ | $[(M([16]aneS_4))_2I](I_5)I$ | 157 s | 2.798 | 0.71 | $I^-\cdot 2I_2$ |
| | (M = Pd, Pt) | 149 m | 2.836 | 0.64 | |
| | | | 3.409 | 0.14 | |
| | | | 3.044 | 0.36 | |
| $I_5^- + I_3^-$ | $[Pd_2Cl_2([18]aneN_2S_4)]_{1.5}I_5(I_3)_2$ | 168 w | 2.775 | 0.75 | $I^-\cdot 2I_2$ |
| | | 147 w | 2.847 | 0.62 | |
| | | | 3.045 | 0.36 | |
| | | | 3.349 | 0.16 | |
| | | 138 w | 2.904(2.929) | 0.53(0.50) | $I_3^-$ (sl. asymm.) |
| | | 108 s | 2.959(2.948) | 0.46(0.47) | |
| $I_3^-$ | $[Pd_2Cl_2([18]aneN_2S_4)](I_3)_2$ | 130 s | 2.865 | 0.59 | $I_3^-$ (asymm.) |
| | | 108 w | 2.989 | 0.42 | |
| $I_5^- + I_2$ | $[RhCl_2[16]aneS_4)]I_5I_2$ | 172 s | 2.732 | 0.85 | $I_2 + I_3^-\cdot I_2$ |
| | | | 2.752 | 0.80 | |
| | | 126 w | 2.962 | 0.45 | $I_3^-$ (asymm.) |
| | | 107 w | 2.884 | 0.56 | |
| $I_9^-$ | $[K([15]aneO_5)_2]I_9$ | 180 br s | 2.716 | 0.88 | $I_2$ |
| | | | 2.728 | 0.85 | |
| | | | 2.740 | 0.83 | |
| | | 131 w | 2.874 | 0.58 | $I_3^-$ (asymm.) |
| | | 109 w | 2.978 | 0.43 | |

[a] For polyiodides not described herein see refs 19 and 39. [b] Note: br = broad s = strong, m = medium, w = weak, br = broad. [c] The I–I bond order (*n*) has been calculated using the equation: $d = d_o - c\log n$ ($d_o$ = 2.67 Å, $c$ = 0.85) ref. 19. [d] $(EtNH_2)$dtl = 3,5-bis(ethylamino)-1,2-dithiolylium. [e] moH = morpholinium. [f] modtc = morpholinecarbodithioato. [g] bntSeMe = *N*-methylbenzothiazole-2(3*H*)-selone. [h] $mo_2$ttl = 3,5-bis(*N*-morpholinio)-1,2,3-trithiolate.

and $E_g$ modes, respectively. It is important to note that the Raman spectrum of $[Ag([18]aneS_6)]I_7$ is very similar to that recorded for $[(butSeMe)_2I]I_7$ in which the $I_7^-$ unit has an approximate $C_{3v}$ symmetry describable as $[I^-\cdot(I_2)_3]$. In the $C_{3v}$ point group the stretching vibrations of the three individual $I_2$ molecules combine to give normal modes of $A_1$ + E type. A slight distortion of the symmetry from $C_{3v}$ to $C_s$ may redistribute the contribution of the individual $I_2$ groups, the shorter $I_2$ unit giving a greater contribution to the higher frequency band, and the longer $I_2$ units to the lower frequency band.[5]

Similarly, the case of the $I_5^-$ ion with a $C_{2v}$ symmetry in $[Ag([9]aneS_3)_2]I_5$ can be tackled; the vibrations of the two individual $I_2$ units combine to give normal modes of the $A_1 + B_2$ types. A lowering of the symmetry due to different bond distances for the two perturbed $I_2$ units will increase the energy of the higher and lower the energy of the lower energy stretch.

The extended interactions in the crystal lattice can play an important role in determining the intensities of the FT-Raman bands. Indeed, quite surprisingly in the Raman spectrum of $[Pd_2Cl_2([18]aneN_2S_4)]_{1.5}I_5(I_3)_2$, a lower intensity is found for the peaks due to the perturbed $I_2$ molecules compared to the intensity of the peak assigned to the symmetric stretch of the $I_3^-$ units at 108 $cm^{-1}$.

The FT Raman spectra have also been recorded after mixing solutions of the metal complex and diiodine for several hours. The presence of only the broad peak at around 208 $cm^{-1}$ due to $I_2$ in solution clearly indicates that the template effect of the metal macrocyclic complexes takes place during the crystallization process.

## 4 Conclusions

Although extended oligomeric anionic polyiodides are a well established aspect of the chemistry of $I_2$, no attempts have been made previously to control their geometrical features by tuning the size, shape and charge of the cation partner. On the grounds that large anions tend to be stabilised by large cations, we thought that thioether macrocyclic complexes could be useful templating agents for extented polyiodide arrays: they are relatively inert species and their size, shape and charge can be varied readily through changes of the metal ion, the macrocyclic crown and co-ligands. The results presented in this review clearly show our aim partially fulfilled. Undoubtedly, the shape of the cation plays the major role on the overall templating effect. For example, essentially spherical cations such as $[Ag([18]aneS_6)]^+$ and $[K([15]aneO_5)_2]^+$ appear to be good template agents for cage-like polyiodide arrays. However, long-range S···I and metal···I contacts can tip the balance and lead to different geometrical motifs in the resulting polyiodide arrays. The synthetic approach also has its own importance; the use of an excess of $I_2$ instead of preformed $I_3^-$ or $I_5^-$ salts is recommended in the first instance, with the preferred polyiodide nuclearity being formed by self-assembly. Once the preferred nuclearity is known, high yielding routes can be developed by the use of preformed $I_3^-$ or $I_5^-$ salts and titration with $I_2$. The use of thioether macrocyclic and related protected complexes appears to be a promising way to template-synthesize extended polyiodide matrices and to control their geometrical features. Moreover, these results suggest that shape-selectivity can be achieved *via* template synthesis of, for example, helicate polyanions at helicate metal-complexes and related hosts.

## 5 Acknowledgements

We thank the EPSRC and the University of Nottingham for support. Figures 4, 5, 12 and 16 have been reproduced with permission.

## 6 References

1 K.-F. Tebbe, in *Polyhalogen cations and Polyhalide Anions. Homoatomic Rings, Chains and Macromolecules of Main-Group Elements*, ed. A. L. Rheingold, Elsevier, Amsterdam, 1977, p. 551.
2 J. R. Ferraro and J. M. Williams, in *Introduction to Synthetic Electrical Conductors*, Academic Press, New York, 1987.
3 T. L. Hendixson, M. A. ter Horst and R. A. Jacobson, *Acta Crystallogr. Sect. C*, 1991, **47**, 2141.
4 R. Poli, J. C. Gordon, R. K. Khanna and P. E. Fanwick, *Inorg. Chem.*, 1992, **31**, 3165.
5 F. Demartin, P. Deplano, F. A. Devillanova, F. Isaia, V. Lippolis and G. Verani, *Inorg. Chem.*, 1993, **32**, 3694.
6 M. W. Renner, K. M. Barkigia, Y. Zhang, C. J. Medforth, K. M. Smith and J. Fajer, *J. Am. Chem. Soc.*, 1994, **116**, 8582.
7 P. C. Junk, L. R. MacGillivray, M. T. May, K. D. Robinson and J. L. Atwood, *Inorg. Chem.*, 1995, **34**, 5395.
8 P. K. Hon, T. C. W. Mak and J. Trotter, *Inorg. Chem.*, 1979, **18**, 2916.
9 A. J. Jircitano, M. C. Colton and K. B. Mertes, *Inorg. Chem.*, 1981, **20**, 890.
10 U. Behrens, H. J. Breunig, M. Denker and K. H. Ebert, *Angew. Chem., Int. Ed. Engl.*, 1994, **33**, 987.
11 K.-F. Tebbe, M. El Essawi and S. Abd El Khalik, *Z. Naturforsch., Teil B*, 1995, **50**, 1429 and references therein.
12 W. J. James, R. J. Hach, D. French and E. R. Rundle, *Acta Crystallogr.*, 1955, **8**, 814.
13 F. Bigoli, F. Demartin, P. Deplano, F. A. Devillanova, F. Isaia, V. Lippolis, M. L Mercuri, M. A. Pellinghelli and E. F. Trogu, *Inorg. Chem.*, 1996, **35**, 3195.
14 K.-F. Tebbe and A. Kavoosian, *Z. Naturforsch., Teil B*, 1993, **48**, 438.
15 K.-F. Tebbe and T. Gilles, *Z. Anorg. Allg. Chem.*, 1996, **622**, 138.
16 F. Bigoli, M. A. Pellinghelli, G. Crisponi, P. Deplano and E. F. Trogu, *J. Chem. Soc., Dalton Trans.*, 1985, 1349.
17 K.-F. Tebbe and T. Farida, *Z. Naturforsch., Teil B*, 1995, **50**, 1440.
18 K.-F. Tebbe and R. Buchem, *Angew. Chem., Int. Ed. Engl.*, 1997, **36**, 1345.
19 P. Deplano, F. A. Devillanova, J. R. Ferraro, M. L. Mercuri, V. Lippolis and E. F. Trogu, *Appl. Spectrosc.*, 1994, **48**, 1236 and refs. therein.
20 F. H. Herbstein, G. M. Reisner and W. Schwotzer, *J. Inclusion Phenom.*, 1985, **3**, 173.
21 K.-F. Tebbe and T. Farida, *Z. Naturforsch., Teil B*, 1995, **50**, 1685.
22 K.-F. Tebbe and M. Bittner, *Z. Anorg. Allg. Chem.*, 1995, **621**, 218.
23 E. E. Havinga and E. H. Wiebenga, *Acta Crystallogr.*, 1958, **11**, 733.
24 O. Hassel and H. Hope, *Acta Chem. Scand.*, 1961, **15**, 407.
25 J. C. Slater, *Acta Crystallogr.*, 1959, **12**, 197.
26 A. J. Jircitano and K. B. Mertes, *Inorg. Chem.*, 1983, **22**, 1828.
27 A. J. Blake, F. Cristiani, F. A. Devillanova, A. Garau, L. M. Gilby, R. O. Gould, F. Isaia, V. Lippolis, S. Parsons, C. Radek and M. Schröder, *J. Chem. Soc., Dalton Trans.*, 1997, 1337 and references therein.
28 A. J. Blake and M. Schröder, *Adv. Inorg. Chem.*, 1990, **35**, 1 and references therein.
29 A. J. Blake, D. Collison, R. O. Gould, G. Reid and M. Schröder, *J. Chem. Soc., Dalton Trans.*, 1993, 521.
30 A. J. Blake, R. O. Gould, W.-S. Li, V. Lippolis, S. Parsons, C. Radek and M. Schröder, *Inorg. Chem.*, submitted.
31 S. Menon and M. V. Rajasekharan, *Inorg. Chem.*, 1997, **36**, 4983.
32 A. J. Blake, R. O. Gould, S. Parsons, C. Radek and M. Schröder, *Angew. Chem., Int. Ed. Engl.*, 1995, **34**, 2374.
33 A. J. Blake, W.-S. Li, V. Lippolis, S. Parsons and M. Schröder, *Acta Crystallogr., Sect C.*, 1998, **54**, 299 and papers in the press.
34 A. J. Blake, V. Lippolis, S. Parsons and M. Schröder, *Chem. Commun.*, 1996, 2207.
35 A. J. Blake, M. J. Bywater, R. D. Crofts, A. M. Gibson, G. Reid and M. Schröder, *J. Chem. Soc., Dalton Trans.*, 1996, 2979.
36 A. J. Blake, W.-S. Li, V. Lippolis, S. Parsons, C. Radek and M. Schröder, *Angew. Chem.*, 1998, **37**, 293.
37 A. J. Blake, G. Reid and M. Schröder, *J. Chem. Soc., Dalton Trans.*, 1990, 3363.
38 F. Demartin, F. A. Devillanova, F. Isaia, V. Lippolis and G. Verani, *Inorg. Chim. Acta*, 1997, **255**, 203 and references therein.
39 P. Deplano, F. A. Devillanova, J. R. Ferraro, F. Isaia, V. Lippolis and M. L. Mercuri, *J. Appl. Spectrosc.*, 1992, **11**, 1625 and references therein.

*Received 19th June 1997*
*Accepted 5th January 1998*